Journal of Marine Research, 45, 813–827, 1987

Continental-shelf-scale model of the Leeuwin Current

by R. O. R. Y. Thompson[1]

ABSTRACT

A simple model is presented for the poleward eastern boundary current (the Leeuwin Current) off Western Australia. For continental-shelf length-scales and seasonal time-scales, the advective and time-derivative terms are small, and water flows onto the shelf until a sufficient cross-shelf pressure gradient is set up to push the same flux back. In a rotating system, the return flux takes place in a frictional (Ekman) layer at the bottom, and is synonymous with a near-bottom longshore current v_B, from

$$-c_D|v_B|v_B = \int_{-H}^{0} \frac{1}{\rho}\frac{\partial p}{\partial y}\,dz + u_*^2,$$

which is equatorward close to shore, but poleward past the 40 m isobath. If the mixed layer is deep enough, there is no upwelling, despite the upwelling-favorable winds. The light surface water is pushed down, causing a baroclinic shear enhancing the poleward current. Advection causes an intense sloping density, salinity, and tracers front. Observed u_*^2 and p_y from Western Australia predict v_B to be poleward in early winter at about 0.2 m s^{-1}, and near zero in summer. The sea-level-slope $g\eta_y$ correlates highly ($r = 0.9$) with the wind-stress u_*^2, with a regression of (100 m)$^{-1}$, both along Western Australia and western North America.

1. Introduction

Cresswell and Golding (1980) and Thompson (1984) observed a poleward surface flow (the Leeuwin Current) over the outer Western Australian shelf from 22S to 34S in autumn and winter, despite a strong equatorward wind. The current is strongest near the shelf break, is about 100 km wide and 2000 km long, and is strongest in early winter (May), when it is 0.6 m s^{-1} poleward at the surface dropping to zero near 150 m depth and reversing to 0.4 m s^{-1} equatorward near 300 m depth, according to Thompson (1984). The longshore windstress is near 0.10 N m^{-2} in summer, dropping to near zero in winter (Godfrey and Ridgway, 1985). The sea level drops about 0.33 m between 20S and 32S (Hamon, 1965; Thompson, 1984; Godfrey and Ridgway, 1985) along 111E, which is a geopotential gradient of

$$A = -g\eta_y = -p_y/\rho = 2.3 \times 10^{-6}\ \text{m s}^{-2} \qquad (1.1)$$

1. P. O. Box 24, Lindisfarne, Tasmania, 7015, Australia.

poleward. Away from the continent, this poleward push is constrained by rotation from causing a poleward flow; it is rotated to an eastward flow of

$$u = -\frac{1}{f}\frac{p_y}{\rho} = \frac{A}{f} \simeq -0.04 \text{ m s}^{-1}. \tag{1.2}$$

How does the presence of the continent break this geostrophic constraint and allow a poleward current? Thompson (1984) observed that it must, but did not venture to explain how. Here it is postulated that bottom friction does the breaking.

2. Theory

Let the y-axis be along-shelf and poleward, and the x-axis offshelf (westward for Western Australia). A basic scale imposed will be (1.1), and consequently (1.2) gives the offshore velocity scale:

$$U = \frac{A}{|f|}. \tag{2.1}$$

If we look for a frictional term $\rho c_D V^2$ to be big enough to match p_y acting over a shelf depth H, then the long-shore-velocity scale is

$$V = \left(\frac{AH}{c_D}\right)^{1/2}, \tag{2.2}$$

which can be much larger than (2.1). The velocity scale (2.2) and the acceleration scale A from (1.1) define a time-scale V/A—a few days—for the velocity to build up to a magnitude where friction can balance the driving. This time-scale and the velocity-scale define a frictional length-scale H/c_D. Now for the crucial scaling assumption: the longshore length-scale L is continental or gyre-sized so:

$$\epsilon = \frac{H}{c_D L} \ll 1. \tag{2.3}$$

This scaling assumption means that the model refers to longshore averages, not point observations.

The full along-shore (y) momentum equation is

$$\frac{\partial v}{\partial t} + u\frac{\partial v}{\partial x} + v\frac{\partial v}{\partial y} + w\frac{\partial v}{\partial z} = -fu + \frac{1}{\rho}\frac{\partial \tau}{\partial z} - \frac{1}{\rho}\frac{\partial p}{\partial y}. \tag{2.4a}$$

At $z = 0$ (the surface),

$$\tau = -\overline{\rho w' v'} = -\rho u_*^2 \lesssim 0.1 \text{ N m}^{-2}. \tag{2.4b}$$

This windstress is spread over a mixed layer whose depth is of the order of 50 m or more for the Leeuwin in winter (Thompson, 1984), so the windstress term in (2.4) is nowhere

dominant over the pressure and Coriolis terms. At $z = -H$ (the bottom),

$$\tau = -\rho c_D |v_B| v_B, \tag{2.4c}$$

where v_B is the velocity just above the bottom frictional layer.

The x (offshore) derivative scale $\lambda = NH/f$ defines a Rossby number

$$R_o = \frac{V}{f\lambda}. \tag{2.5}$$

Since $NH/f \lesssim (10^{-2}\,\mathrm{s}^{-1}\ 200\ \mathrm{m})/0.6 \times 10^{-4}\,\mathrm{s}^{-1} = 30\ \mathrm{km}$, R_o will be small. This is convenient, though not crucial. The vertical velocity scale W will then be

$$W = \frac{H}{\lambda} U. \tag{2.6}$$

If the forcing were abruptly switched on, the response would occur on the acceleration time-scale V/A outlined above. This paper will look at time-scale $T \gg V/A$, so we see an equilibrium response to the forcings τ and p_y. Define

$$\sigma = \frac{V}{AT}. \tag{2.7}$$

With these scalings, the nondimensional form of (2.4) is

$$\sigma v_t + R_o(uv_x + wv_z) + \epsilon v v_y = u + \frac{\partial \tau}{\partial z} - p_y. \tag{2.8}$$

Keeping (2.4) in dimensional form, but dropping the terms which are small in (2.8), the zero-order longshore momentum equation is just

$$-fu = \frac{1}{\rho}\left(\frac{\partial p}{\partial y} - \frac{\partial \tau}{\partial z}\right). \tag{2.9}$$

Now scale the continuity equation

$$\frac{\partial u}{\partial x} + \frac{\partial v}{\partial y} + \frac{\partial w}{\partial z} = 0. \tag{2.10}$$

The ratio of the second term to the first is of order

$$\mu = \frac{V}{U}\frac{\lambda}{L} = \left(\frac{H}{Ac_D}\right)^{1/2} f\frac{\lambda}{L} = \epsilon^{1/2}\frac{NH}{(AL)^{1/2}}, \tag{2.11}$$

so if the length scale L is large, or the depth-scale H small, then the longshore divergence v_y cannot balance the onshore flux, and that flux must return through the bottom Ekman layer. The assumption that L is large enough that ϵ and μ are small is

the chief simplifier of the theory. Dropping the term $0(\mu)$ in (2.10) gives

$$\frac{\partial u}{\partial x} + \frac{\partial w}{\partial z} = 0. \tag{2.12}$$

We can now integrate (2.12) from the surface [$z = 0$] where $w = 0$ to the bottom [$z = -H(x)$] where $u = w = 0$, so:

$$\begin{aligned} 0 &= \int_{-H}^{0} \left(\frac{\partial u}{\partial x} + \frac{\partial w}{\partial z}\right) dz = \int_{-H}^{0} \frac{\partial u}{\partial x}\, dz + 0 - 0 \\ &= \int_{-H}^{0} \frac{\partial u}{\partial x}\, dz = \frac{\partial}{\partial x}\int_{-H}^{0} u dz - 0 \cdot \frac{dH}{dx} = \frac{\partial}{\partial x}\int_{-H}^{0} u dz. \end{aligned} \tag{2.13}$$

Now substitute u from (2.9), so

$$\begin{aligned} 0 &= \frac{\partial}{\partial x}\int_{-H}^{0} \frac{-1}{\rho f}\left(\frac{\partial p}{\partial y} - \frac{\partial \tau}{\partial z}\right) dz \\ &= -\frac{1}{f}\frac{\partial}{\partial x}\left[\int_{-H}^{0} \frac{1}{\rho}\frac{\partial p}{\partial y}\, dz - \frac{1}{\rho}(\tau(0) - \tau(-H))\right]. \end{aligned} \tag{2.14}$$

Now integrate (2.14) out from the shore, where $H = 0$, so

$$0 = \int_{-H}^{0} \frac{1}{\rho}\frac{\partial p}{\partial y}\, dz + u_*^2 + c_D |v_B| v_B \tag{2.15}$$

determines v_B, the longshore velocity just above the bottom frictional layer. A nice feature is that it shows that v_B is not sensitive to baroclinicity nor details of the absorption of the windstress, such as the depth of the wind-mixed layer. There may be some influence of surface waves or tides on c_D, but otherwise v_B is determined quite robustly in terms of the large scale imposed parameters p_y and u_*^2.

The first term in (2.15) goes to zero as $H \to 0$, so in shallow water the current always goes with the wind (equatorward):

$$v_B \to -u_*/c_D^{1/2} \simeq -30u_*. \tag{2.16}$$

Going offshore, the current continues to move equatorward until reaching that isobath $H(x) = H_*$ where the total (vertically integrated) longshore pressure gradient overcomes the total windstress, or

$$\int_{-H_*}^{0} \frac{1}{\rho}\frac{\partial p}{\partial y}\, dz = u_*^2, \tag{2.17}$$

If this is not too deep, $(1/\rho)\, \partial p/\partial y \simeq A$, so

$$H_* \simeq \frac{u_*^2}{A} \lesssim \frac{10^{-4}\ \mathrm{m^2\ s^{-2}}}{2.3 \times 10^{-6}\ \mathrm{m\ s^{-2}}} = 40\ \mathrm{m}. \tag{2.18}$$

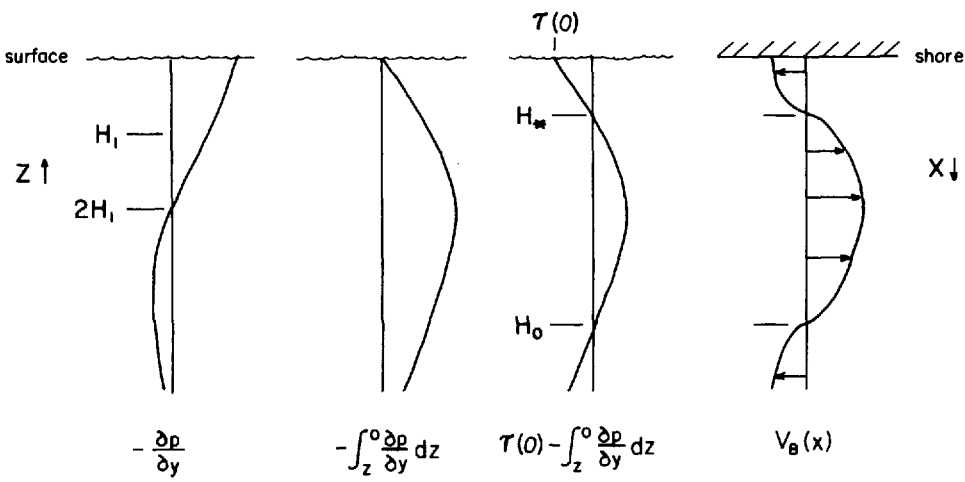

Figure 1. Vertical distributions of geopotential gradient and resultant $v_B(x)$. Poleward is to right in each profile.

Beyond this isobath, the bottom current goes against the wind. The maximum v_B occurs at the isobath (depth) where $p_y = 0$: though driven by the pressure gradient, v_B is strongest where that driving vanishes! Figure 1 is a sketch illustrating the calculation of $v_B(x)$ for reasonable $p_y(z)$ and u_*^2.

Now for the cross-shelf momentum balance,

$$\frac{\partial u}{\partial t} + u\frac{\partial u}{\partial x} + v\frac{\partial u}{\partial y} + w\frac{\partial u}{\partial z} = fv - \frac{1}{\rho}\frac{\partial p}{\partial x} - \frac{1}{\rho}\frac{\partial \tau^{(x)}}{\partial z}. \tag{2.19}$$

Above the Ekman layer, the pressure gradient scale is

$$\left|\frac{1}{\rho}\frac{\partial p}{\partial x}\right| = fV. \tag{2.20}$$

The Reynolds stress $\tau^{(x)}$ is small in the interior, but must be important in the Ekman layer (of thickness δ) since u, v, and w all go to zero at the bottom, but $\partial p/\partial x$ does not, so

$$\left|\frac{1}{\rho}\frac{\partial p}{\partial x}\right| = \frac{\left|\frac{1}{\rho}\tau^{(x)}\right|}{\delta} = \frac{c_D V^2}{\delta}. \tag{2.21}$$

With (2.20), this implies

$$\delta = \frac{c_D V}{f}. \tag{2.22}$$

Above the bottom Ekman layer, the small terms in (2.19) can be neglected:

$$fv = \frac{1}{\rho}\frac{\partial p}{\partial x}. \tag{2.23}$$

3. Reprise

Now that the model is assembled, let's see how well it fits the Leeuwin Current, remembering that averaging to continental and seasonal scales precludes consideration of mesoscale or transient phenomena.

The acceleration potential pushing the motion is of order $A = 2.3 \times 10^{-6}$ m s^{-2} from (1.1), so the velocity scale

$$V = \left(\frac{AH}{c_D}\right)^{1/2} \simeq \left(\frac{2.3 \times 10^{-6}}{1.5 \times 10^{-3}}\right)^{1/2} = 0.4 \text{ m s}^{-1}, \tag{3.1}$$

which is indeed the sort of velocity observed by Thompson (1984). The Western Australian shelf tends nearly north-south under nearly uniform winds and geopotential gradient from North West Cape (22S) to Cape Leeuwin (34S), so the longshore length scale L could be as much as 1500 km. The shelf is not more than $H = 200$ m deep, so

$$\epsilon = \frac{H}{c_D L} \simeq \frac{0.2 \text{ km}}{1.5 \times 10^{-3} \times 1500 \text{ km}} = 0.1 \tag{3.2}$$

is small. The hydrographic sections across the current of Thompson (1984) suggest a horizontal derivative scale of

$$\lambda \simeq 30 \text{ km}, \tag{3.3}$$

so in (2.5),

$$R_o = \frac{V}{f\lambda} \simeq \frac{0.4}{0.6 \times 10^{-4} \times 3 \times 10^4} = 0.2, \tag{3.4}$$

which is reasonably small. For an annual period, the time-scale $T = \text{year}/2\pi = 5 \times 10^6$ sec, so in (2.7)

$$\sigma = \frac{V}{AT} \simeq \frac{0.4}{2.3 \times 10^{-6} \times 5 \times 10^6} \simeq 0.04, \tag{3.5}$$

which is indeed small in (2.8). As to the neglect of longshore divergence in the continuity equation, the ratio (2.11) of $|v_y|$ to $|u_x|$ is

$$\mu = \frac{V}{U}\frac{\lambda}{L} \simeq \frac{0.4}{0.04}\frac{30}{1500} = 0.2. \tag{3.6}$$

All of the quantities neglected in the theory are small for the Leeuwin, so the theory

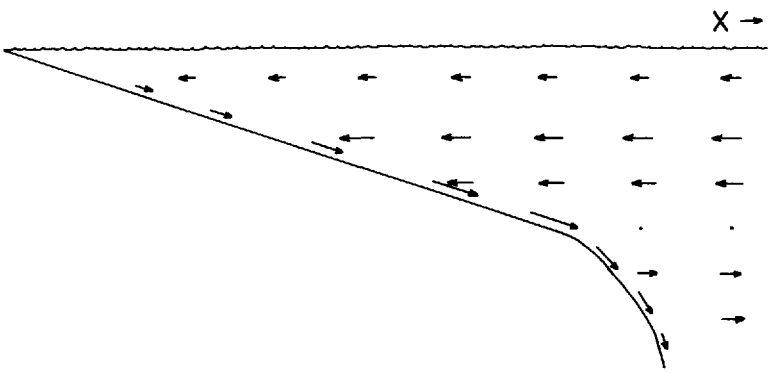

Figure 2. Cross-shelf circulation. Horizontal flow is unaffected by the presence of the shelf until actually hitting the frictional bottom (Ekman) layer.

may apply. For instance, the bottom Ekman layer thickness from (2.22),

$$\delta = \frac{c_D V}{f} \simeq \frac{(1.5 \times 10^{-3})\ 0.4\ \text{m/s}}{0.6 \times 10^{-4} \times \text{s}^{-1}} = 10\ \text{m}, \tag{3.7}$$

is a small fraction of the shelf depth. Above this thin layer, the onshore velocity (2.9) is undisturbed from its open ocean value; u does not even know about the shelf until it runs right into the Ekman layer! (This is sketched in Figure 2.) The cross-shelf pressure gradient necessary to push this flux back (through the thin Ekman layer) also causes a longshore current via geostrophy [Eq. (2.23)].

4. Seasonal sea-level and velocity changes

It will be convenient to express the momentum balance (2.15) in terms of sea-surface slope, η_y. At the surface, $p_y = \rho g \eta_y$, but the shallowness of the thermocline in the tropics causes p_y to shrink rapidly with depth; to zero by 150 m, and reversed by 200 m depth, according to Thompson (1984) or Godfrey and Ridgway (1985). Therefore, write

$$\int_{-H}^{0} \frac{1}{\rho} \frac{\partial p}{\partial y}\, dz = g \eta_y H_1, \tag{4.1}$$

where $H_1 \simeq H$ for shallow water (say $H \lesssim 50$ m), but is limited to $H_1 \lesssim \frac{1}{2}$ (150 m) for deeper H, as the steric anomaly cancels out. More precisely, Ken Ridgway (private communication) has calculated geopotential anomaly fields off Western Australia at 100 m depth intervals. By differencing his inshore point off North West Cape (22S) and off Fremantle (32S), one finds $-(1/\rho)p_y = A = 1.5 \times 10^{-6}\ \text{m s}^{-2}$ at $z = 0$, $0.5 \times 10^{-6}\ \text{m s}^{-2}$ at $z = -100$ m, and negative at $z = -200$ m. A linear interpolation then

Table 1. Monthly average windstress and sea-level along Western Australian.

Symbol:	u_*^2	Sea-level Fremantle	Sea-level Carnarvon	$\Delta\eta$	A	u_*^2/A	AH_1	$AH_1-u_*^2$	ν_B
Units:	10^{-4} m^2/s^2	m	m	m	10^{-6} m s^{-2}	m	10^{-4} m^2/s^2	10^{-4} m^2/s^2	m/s
Jan	1.0	1.72	1.84	−.12	1.4	70	1.0	0.0	.00
Mar	1.0	1.78	1.93	−.15	1.8	50	1.3	0.3	.15
May	0.2	1.95	2.02	−.07	0.9	20	0.6	0.4	.17
July	0.0	1.89	1.93	−.04	0.5	0	0.3	0.3	.15
Sept	0.4	1.76	1.81	−.05	0.6	70	0.4	0.0	.00
Nov	0.9	1.71	1.81	−.10	1.2	70	0.8	−0.1	−.02

gives

$$H_1 = 100 \frac{0.5}{1/2(1.5)} = 70 \text{ m}. \tag{4.2}$$

Farther offshore, one finds that A increases to 3×10^{-6} m s^{-2} and H_1 to 100 m, but the near-shelf values seem more relevant. Putting (4.1) in (2.15) gives

$$c_D |v_B| v_B = -gH_1\eta_y - u_*^2. \tag{4.3}$$

There is a strong seasonal variation in the windstress along Western Australia. In Table 1 are tabulated the monthly-average windstress equatorward along the shelf between Cape Leeuwin (34S) and Carnarvon (24S), and the monthly-average sea levels at Fremantle (32S) and Carnarvon, all taken from Godfrey and Ridgway (1985). From these data, the terms in (4.3) were computed, using $H_1 = 70$ m, $c_D = 1.5 \times 10^{-3}$, and $\Delta y = 830$ km.

A strong relationship between windstress and sea-level slope was found, and plotted in Figure 3. The correlation is $r = 0.9$, the intercept (for $u_*^2 = 0$) is $g\eta_y = -0.5 \times 10^{-6}$ m s^{-2}, and the slope of the regression (100 m)$^{-1}$.

This relationship between wind-stress and sea-level slope seems striking enough to check whether it may not occur elsewhere. Hickey and Pola (1983) give monthly mean sea levels and Bakun winds in their Figure 4. For Southern California (San Diego to San Francisco), the correlation is $r = 0.44$ (for $n = 12$ monthly means) with regression coefficient 1.0×10^{-2} m^{-1} = (100 m)$^{-1}$. For Northern California (San Francisco to Crescent City), the correlation is $r = 0.93$ with regression coefficient 0.9×10^{-2} m^{-1} = (110 m)$^{-1}$. For Oregon-Washington (Crescent City to Neah Bay), the correlation is $r = 0.80$ with regression coefficient 1.0×10^{-2} m^{-1} = (100 m)$^{-1}$.

5. Advection

Table 1 predicts currents for depths of order 100 m over the shelf of Western Australia, using values from Godfrey and Ridgway (1985). In spring and early summer (September to January), the current is predicted to be nearly still, so the shelf water may be expected to equilibrate to the local latitudinal values in markers such as temperature, salinity, nutrients, and fish species. Table 1 predicts that the current becomes poleward about February, and in March moves the outer shelf water poleward about (0.15 m s^{-1}) (31 days) $\simeq$ 400 km. If it moved half this far in February, the water which was at North West Cape in early February will have moved some 600 km south by the end of March, and will reach the shelf off Rottnest Island about the end of April. Therefore, the salinity off Rottnest should drop toward tropical values about the end of April—as was observed by Cresswell and Golding (1980), who also found that the water temperature stopped dropping, despite winter coming on.

The values of p_y used by Godfrey and Ridgway (1985) were extrapolated across the

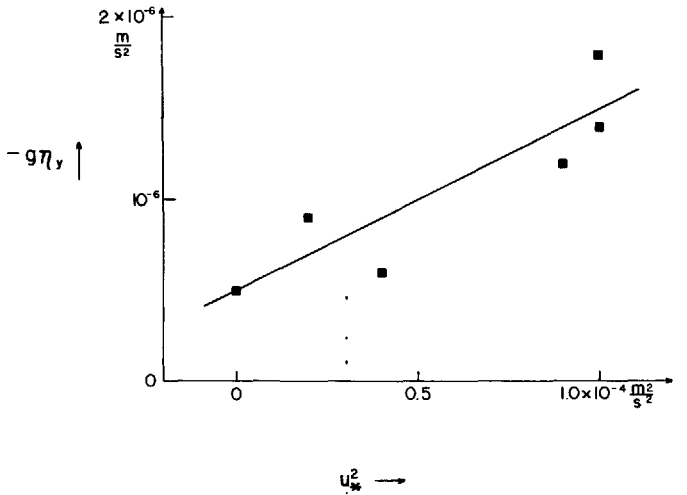

Figure 3. Sea-level slope between Fremantle and Carnarvon plotted versus equatorward windstress, from Table 1. The line is the least-squares best fit, $-g\eta_y = 0.5 \times 10^{-6}$ m s^{-2} + $u_*^2/100$ m.

shelf, and are much smaller than the shelf-edge p_y of Thompson (1984). If Thompson's value of A is used, the current is predicted to flow poleward all year.

6. Downwelling

The flow down the Ekman layer in Figure 2 is downwelling. Unlike v_B its calculation depends not just on $\tau(0)$, but on τ_z. For simple illustration, use a "slab" mixed layer, so

$$\frac{1}{\rho}\frac{\partial \tau}{\partial z} = \begin{pmatrix} u_*^2/h, & \text{if } -h < z < 0 \\ 0, & \text{if } z < -h \\ & (\text{and } z > -H + \delta) \end{pmatrix}, \tag{6.1}$$

where the mixed-layer depth h is small enough ($h \lesssim H_1$) so $\rho^{-1} p_y (= -A)$ is independent of z. These make (2.9) very simple:

$$u = \frac{1}{-f}\begin{pmatrix} -A + \dfrac{u_*^2}{h}, & \text{if } -h < z < 0 \\ -A \quad , & \text{if } z < -h \end{pmatrix}, \tag{6.2}$$

above the bottom Ekman layer. An immediate deduction from (6.2) is that the flow is onshore in the mixed layer if $u = -A + u_*^2/h < 0$, or if the nondimensional

parameter

$$\frac{u_*^2}{Ah} < 1. \tag{6.3}$$

If the mixed layer is deep enough, there is *no* upwelling, even from a "nutrient depleted surface layer," despite the upwelling favorable wind! Noting that H_* in (2.17) is u_*^2/A here,

$$h > H_* \rightarrow \text{no upwelling.} \tag{6.4}$$

For the Leeuwin in May, $A = 0.9 \times 10^{-6}$ m s^{-2} and $u_*^2 = 0.2 \times 10^{-4}$ m^2 s^{-2} according to the values of Godfrey and Ridgway (1985) used in Table 1, and $h > 50$ m according to Rochford (1969), so

$$h > 50 \text{ m} > 22 \text{ m} = u_*^2/A, \tag{6.5}$$

and (6.4) predicts *no* upwelling; there should be downwelling from the surface strengthening downward to the base of the thermocline.

For the Leeuwin in summer, Godfrey and Ridgway's (1985) values for A and u_*^2 predict upwelling from a depth of 70 m. However, Thompson's (1984) value for A still predicts no upwelling if $h \geq 25$ m in summer.

7. Density structure

So far, stratification has entered only insofar as it confined windstress to a surface mixed layer. Now for an attempt to extend the model to predict robust features of the density structure and baroclinic shear.

The downwelling sketched in Figure 2 implies an offshore/downward flux in the bottom Ekman layer. This flux for the Leeuwin is (from Table 1) of order 0.6 m^2 s^{-1} over an Ekman thickness $\delta \simeq 10$ m, so the cross-shelf speeds are of order $U_e = 0.06$ m s^{-1}! This would seem to mean that a particle originally near shore could traverse the x-scale $\lambda = 30$ km in about five days. However, this will not happen, because five days is very slow compared to the stratification adjustment time N^{-1}, so the forcing is too slow to cause overturning. As light water is pushed below its equilibrium level, it interchanges with slightly heavier water above it on a slant slightly less than that of the isopycnal slope, as sketched in Figure 4. Therefore, the water particles themselves will not move down the slope any faster than accumulation moves the isopycnals. Since the lighter water accumulates against the continent, the isopycnals will move down, at a slope η_x, implying a baroclinic shear

$$\frac{\partial v}{\partial z} = -\frac{g}{f\rho_o}\frac{\partial \rho}{\partial x} = -\frac{N^2}{f}\eta_x. \tag{7.1}$$

This feature seems robust: the downwelling will cause a downward tilt of the

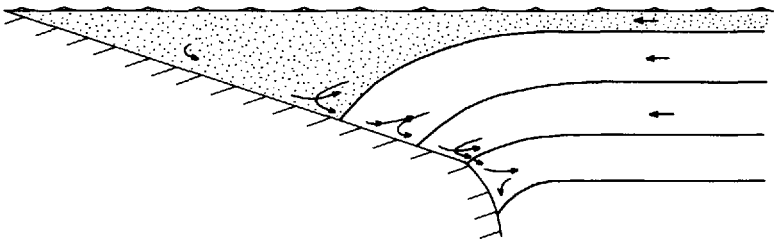

Figure 4. Isopycnal tilts and slant-wise convection caused by downwelling. The stippled area represents the surface water mass, the arrows the particle motions.

isopycnals near the shelf, and consequently a poleward shear of the current above v_B. The poleward Leeuwin Current will be stronger near the surface than near the bottom. Despite being driven from the bottom, the current is *not* bottom trapped.

Despite advection, there will be another robust feature if the imposed u_*^2 and $\partial p/\partial y$ allow a depth H_o where the Ekman flux (and hence v_B) again go to zero, as illustrated in Figure 1. A front will form at H_o since the Ekman flux converges there, bringing isopycnals from both sides close together. This front will be strengthened by longshore advection, since v_B also changes sign at H_o:$v_B > 0$ inshore of H_o brings light tropical water to the inshore side, while $v_B < 0$ offshore of H_o brings heavier extra-tropical water to the offshore side. Therefore, both processes will form a front anchored at the H_o isobath. Since it is a density front in a rotating system, it will slope upward offshore and will sustain a vertical shear. This poleward shear will oppose the equatorward v_B offshore of H_o, so the surface current will be poleward past the H_o isobath, as sketched in Figure 5. The Leeuwin Current will not be bottom-trapped, despite being driven through the bottom Ekman layer.

The Indian Ocean tropical water is relatively fresh, warm, and high in silica (Warren, 1981); the Indian Ocean mid-latitude water is salty and high in oxygen (Rochford, 1969)—so horizontal advection will cause the density front to be also a salinity, silica, and oxyty front. Thompson (1984) observed a very sharp density, salinity, silica, and oxyty front sloping up from the 150 m isobath off Shark Bay—and found $v = 0$ at 150 m by direct measurement.

8. Discussion

The most important physical question for people dealing with a piece of ocean is probably: "Is there upwelling?", for the answer determines whether fish or people will swim in it, and whether there will be rain. The most important theoretical question for physical oceanographers dealing with the Leeuwin is then: "Why is there no upwelling off Western Australia, despite the upwelling-favorable wind?" The theory of the present paper answers: "Because the wind-mixed layer is deeper than the balance depth u_*^2/A, so the pressure gradient overcomes the wind stress." To test this theory

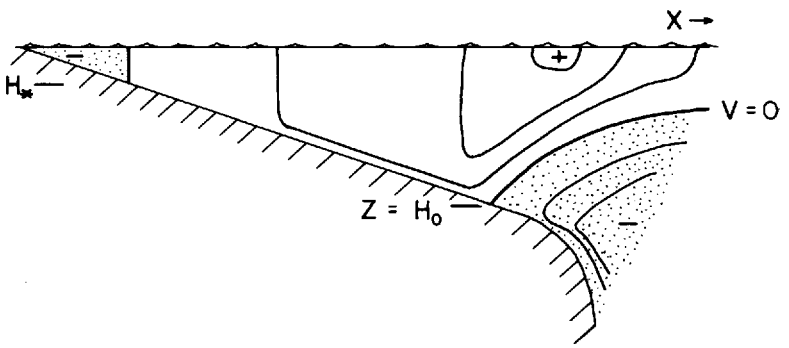

Figure 5. Isopleths of poleward component of flow. The stippled area is negative (equatorward).

requires defining and measuring (1) the mixed layer depth, (2) the longshore wind stress, and (3) the longshore pressure gradient, each over monthly and continental-shelf scales. If all of these can be determined to within 10% and the difference between h and u_*^2/A is more than 20%, then this theory can be meaningfully tested.

The essential feature of the present model is that the balance is in the vertical plane. Deriving the two-dimensional mass balance (2.12) required μ in (2.11) to be small. Due to partial cancellation of the pressure driving by the windstress, Table 1 shows that the relevant scale V is only 0.2 m s^{-1}, so for the Leeuwin

$$\mu = \frac{V\lambda}{UL} \sim \frac{(0.2)(30)}{(0.04)(1500)} = 0.1 \tag{8.1}$$

is rather small. A small part of the onshore mass flux may advect poleward, but most of it can be expected to downwell locally—where "locally" means within distinctly less than $L \simeq 1500$ km.

Huthnance (1984) does present a theory which allows a longshore driving $\partial p/\partial y$, and also involves a two-dimensional mass balance in the vertical plane. Perhaps the major difference in his model from the present one is that Huthnance does not recognize the shallowness of the forcing. The forcing p_y only extends to the thermocline; the vertical scale H_1 is estimated as only 70 m for the Leeuwin, or perhaps 100 m farther out in the Indian Ocean. Huthnance (1984) represents the solution as an infinite sum of vertical moments, but then severely truncates to only the vertical mean (ψ) and the first moment (χ) in the vertical, which is not sufficient to represent a thin boundary layer. (The Leeuwin is only a hundred meters or so deep, very thin compared to the full Indian Ocean depth of 4500 m or so.) This is why Huthnance shrinks the ocean depth to 1 km in his examples. That is still too large to resolve the surface concentration ($H_1 \simeq 70$ m) of the poleward density gradient, which is why Huthnance uses an example value for "surface" density gradient which is an order of magnitude

Table 2. Monthly average wind stress and sea level between San Diego and San Francisco.

Symbol:	u_*^2	$\Delta\eta$	A	u_*^2/A	$AH_1 - u_*^2$	v_B
Units:	10^{-4} m^2/s^2	dyn. m	10^{-6} m/s^2	m	10^{-4} m^2/s^2	m/s
July	.5	−.08	1.2	40	.4	.17
Sep	.5	−.09	1.3	40	.5	.18
Nov	.2	−.06	.8	30	.3	.14
Jan	.2	+.00	−.0	deep	−.2	−.12
Mar	.5	−.02	.3	160	−.3	−.13
May	.6	−.06	.8	75	−.0	−.02

smaller than a realistic value for the mid-latitude Indian Ocean. Huthnance does not include windstress in his model.

Equations similar to (2.15) have been written before now, usually as vertical integrals of (2.4), together with an equivalent-barotropic assumption. In deriving (2.15) here, the water was not assumed to be barotropic. The scaling has been made explicit: the balance (2.15) holds after averaging over a few days and more than a few hundred kilometers along an isobath, and applies to the velocity just above the Ekman layer. It is in convenient form for combining with the vertical shear calculated via (7.1) from the density structure, once that is known.

The theory presented in this paper was developed to explain the wintertime observations of Thompson (1984) and does that quite satisfactorily. No other theory predicts an eastern boundary current flowing against the wind at the surface, flowing with the wind at depth, and possessing a sharp density, salinity, and other properties front between.

A comparison with another boundary current may help to illustrate the application of this model to the Leeuwin. Hickey and Pola (1983) present sea levels and Bakun wind stresses for the west coast of the United States; the data for the San Diego to San Francisco (Δy = 710 km) segment is abstracted in Table 2. The depth H_1 could (and should) be determined from the extensive hydrographic data available to others, but has again been taken as 70 m here, for the illustration. The sea-slope is somewhat smaller for Southern California, so the equatorward wind stress can here cause upwelling all year (except possibly late autumn). Nonetheless, the poleward pressure gradient is strong enough to push a poleward undercurrent in summer and autumn. This is most likely to surface in late autumn, as the wind weakens. Late autumn is also when the surface Leeuwin is strongest.

We found in Section 4 that most of the variance of the monthly mean sea-slope is explained by monthly mean wind-stress. In each of 4 cases, the regression coefficient came out 1.0×10^{-2} (m s^{-2})/(m^2 s^{-2}) = (100 m)$^{-1}$, as if the "adjustment depth" of 100 m has some physical meaning for all 4 different latitude ranges. One possibility is that 100 m is an average shelf-depth, and the shelf-water is acting as would a lake of 100 m depth—a nice, simple behavior!

Perhaps the most original contribution of this paper is noting that the surface ("wind-mixed" or "Ekman") layer may not be of negligible thickness—it can easily be thick enough (6.4) so there is *no* offshore surface flux, despite an upwelling-favorable wind! In fact, this situation holds off Western Australia in winter—and causes downwelling and a poleward eastern boundary current there.

Acknowledgments. Robert L. Smith asked for an explanation of the Leeuwin Current and arranged for the typing and drafting of this attempt; without Bob this paper would not have been started. Adriana (Jane) Huyer and J. Stuart Godfrey also listened and shared their interest with me, which made the work worth doing.

REFERENCES

Cresswell, G. R. and T. J. Golding. 1980. Observations of a south-flowing current in the southeastern Indian Ocean. Deep-Sea Res., *27A,* 449–466.

Godfrey, J. S. and K. R. Ridgway. 1985. The large-scale environment of the poleward-flowing Leeuwin Current, Western Australia: longshore steric height gradients, wind stresses, and geostrophic flow. J. Phys. Oceanogr., *15,* 481–495.

Hamon, B. V. 1965. Geostrophic currents in the southeastern Indian Ocean. Aust. J. Mar. Freshwater Res., *16,* 255–271.

Hickey, B. M. and N. E. Pola. 1983. The seasonal alongshore pressure gradient on the west coast of the United States. J. Geophys. Res., *88,* 7623–7633.

Huthnance, J. M. 1984. Slope currents and 'JEBAR'. J. Phys. Oceanogr., *14,* 795–810.

Rochford, D. J. 1969. Seasonal variation in the Indian Ocean along 110°E. Aust. J. Mar. Freshwater Res., *20,* 1–50.

Thompson, R. O. R. Y. 1984. Observations of the Leeuwin Current off Western Australia. J. Phys. Oceanogr., *14,* 623–628.

Warren, B. A. 1981. Transindian hydrographic section at latitude 18°S: Property distributions and circulation in the South Indian Ocean. Deep-Sea Res., *28A,* 759–788.

Received: *19 November, 1985;* revised: *15 April, 1987.*